Gain predictions for nickel-like gadolinium from a 181-level multiconfigurational distorted-wave collisional-radiative model

W. H. Goldstein and J. Oreg*
High Temperature Physics Division, Lawrence Livermore National Laboratory, Livermore, California 94550

A. Zigler
Department of Plasma Physics, Soreq Nuclear Research Center, Yavne 70600, Israel

A. Bar-Shalom
Nuclear Research Center of the Negev, P.O. Box 9001, Beer Sheva, Israel

M. Klapisch
Racah Institute of Physics, Hebrew University, Jerusalem 91904, Israel
(Received 22 December 1987)

We present small-signal gain coefficients for soft x-ray transitions in nickel-like gadolinium. The gains are predicted by a steady-state collisional-radiative model containing 181 detailed levels, including $n=5$ states. All possible electron collisional transitions among these levels are calculated in the distorted-wave approximation. Our calculations display features that may help to explain discrepancies between design predictions and the gains recently observed in a europium plasma. Also, we identify for the first time $n=3$ to $n=3$ inversions in the nickel-like ion that suggest that the "water window" at 43.7 Å might be reached using such relatively low-Z elements as gadolinium.

I. INTRODUCTION

The recent demonstrations of soft x-ray gain on $n=3$ to $n=3$ transitions in highly stripped neon-like ions[1] has spurred theoretical and experimental interest in other candidates for amplified spontaneous emission. There has been intense speculation on recombination[2,3] and collisional ionization[4] mechanisms, and on helium-like,[2] lithium-like,[3] neon-like,[4] and nickel-like ions.[5,6] Several candidates hold the promise of eventually opening the "water window" at 44 Å, but only one seems headed for success in the near future: collisional pumping of $n=4$ to $n=4$ nickel-like transitions.[5,6]

The nickel-like system is a close relative to the neon-like ion. It has a closed-shell ground state, $(\mathrm{Ne})3s^2 3p^6 3d^{10}$, guaranteeing that appreciable fractions of this charge state will occur in plasma, and it has manifolds of metastable excited levels that can invert with respect to lower-energy, resonantly decaying states. However, the nickel-like ion offers two important advantages. First, $n=4$ to $n=4$ transitions in the soft x-ray regime can be obtained in laser-produced plasma with more modest optical-laser flux (i.e., at lower electron temperatures); and, second, the wavelengths of amplified transitions scale more favorably with Z, than in the neon-like case. For example, gain is predicted[5-7] and observed[8] for a $3d^9 4d\,(J=0)$ to $3d^9 4p\,(J=1)$ at 66 Å in nickel-like europium ($Z=63$) for an input laser fluence of 5.7×10^{13} W/cm^2; in tungsten ($Z=74$), ionized 46 times to nickel-like, this transition occurs within the water window, at 43.1 Å. By comparison, the 206-Å line observed in neon-like selenium ($Z=34$) does not fall below 44 Å until 53 times ionized europium.

As with the neon-like amplifier, success in the nickel-like experiments has been tempered by discrepancies between design predictions and what is actually observed. The neon-like selenium system is predicted to amplify a $J=0$ to $J=1$ transition most strongly,[9] but—until it was recently measured with a lower than expected gain[10]—only $J=2$ to $J=1$ transitions were observed.[1] In the nickel-like Eu experiments, gain is observed in two $J=0$ to $J=1$ lines. But the $J-2$ to $J=1$ lines, expected, in this case, to be stronger,[7] are seen without measurable gain.[8] Thus, in its current incarnation, the "$J=0$" problem has been turned inside out. Z-scaling studies[11,12] and increasingly elaborate kinetics modeling[13,14] have shed some light on the neon-like conundrum, but as yet no completely satisfactory explanation has appeared. The nickel-like anomaly is a further reminder that there are aspects of the atomic physics, population kinetics, and magntohydrodynamics of soft x-ray lasing media that are not yet fully understood.

In this report, we present the small-signal gains predicted for nickel-like gadolinium by an extensive, steady-state model of the nickel-like population kinetics. Our model treats the kinetics of the nickel-like charge state in isolation from other ionization stages—thus dielectronic recombination is neglected. If the neon-like system is taken as a guide, this approximation might appear ill advised.[13,14] But the absence of $J=2$ to $J=1$ amplification in the nickel-like experiment almost certainly indicates that this process is not important under the plasma conditions attained. We will have more to say about this approximation, as well as other processes left out of our model, in Sec. II.

We also presuppose a steady-state plasma at fixed,

homogeneous temperature and density. Our results are accurate only for these idealized, artificial conditions. As a consequence, our gain predictions are meant to be only suggestive, though they feature behavior that lends insight into the physical system. In particular, this approach allows us to investigate the population kinetics of the collisionally excited ion independently of design parameters and transient effects.

A distinct advantage to our approach is the opportunity afforded to identify new behavior that might be obscured in more complete simulations that simultaneously treat the ionization balance or that involve target design choices. For example, we have identified, for the first time, inversions of nickel-like inner-shell transitions. These results intimate that the water window may be reached using relatively low-Z elements, such as nickel-like gadolinium.

Our kinetics model is described in detail in Sec. II followed by the presentation of our results for small-signal gain coefficients. We conclude with a discussion of the significance of the present work.

II. THE MODEL

Our gain calculations are based on a collisional-radiative model of the nickel-like gadolinium ion including the ground state and the 180 levels contained in the configurations $3s^2 3p^6 3d^9 4l$, $3s^2 3p^5 3d^{10} 4l$, $3s 3p^6 3d^{10} 4l$, $l=s,p,d,f$; and $3s^2 3p^6 3d^9 5l$, $l=s,p,d,f,g$. A simplified level diagram for this model is shown in Fig. 1. We have found that the $3d$-$5l$ configurations must be included to accurately predict the population of energetically nearby levels with a hole in the $3s$ or $3p$ orbital. These configurations also contribute population to lower-lying $3d$-$4l$ states through cascades. To illustrate these effects, some of our results will be compared to a 107-level model that does not include the $5l$ levels.

The model includes all $E1$, $M2$, and $E2$ radiative transitions and all electron-impact transitions between levels. The atomic structure and radiative transitions were computed in the relativistic, multiconfiguration parametric potential model with the ANGLAR (Ref. 15) and RELAC (Ref. 16) codes, developed at Hebrew University. Collisional excitation cross sections were computed in the relativistic distorted-wave approximation using methods developed in recent years by several of us.[17] These methods allow us, for the first time, to take into account all possible collisional transitions among the low-lying levels of the nickel-like ion. In this respect, and in the number of levels included, the present model is more complete than previously studied kinetics models.[5-7]

This data was fed into the steady-state collisional-radiative rate equations,

$$\sum_{j=1}^{181} [N_e \mathbf{Q}_{ij}(T_e) + \mathbf{A}_{ij}] n_j = 0 , \tag{1}$$

where N_e is the electron density; T_e is the electron temperature; $\mathbf{Q}_{ij}$, $i \neq j$, is the rate coefficient for a collisional transition from state j to state i; $\mathbf{Q}_{ii} = -\sum_j Q_{ji}$, $\mathbf{A}_{ij}$ is the Einstein coefficient for a radiative transition from state j to state i; and $A_{ii} = -\sum_j A_{ji}$. Equation (1) was

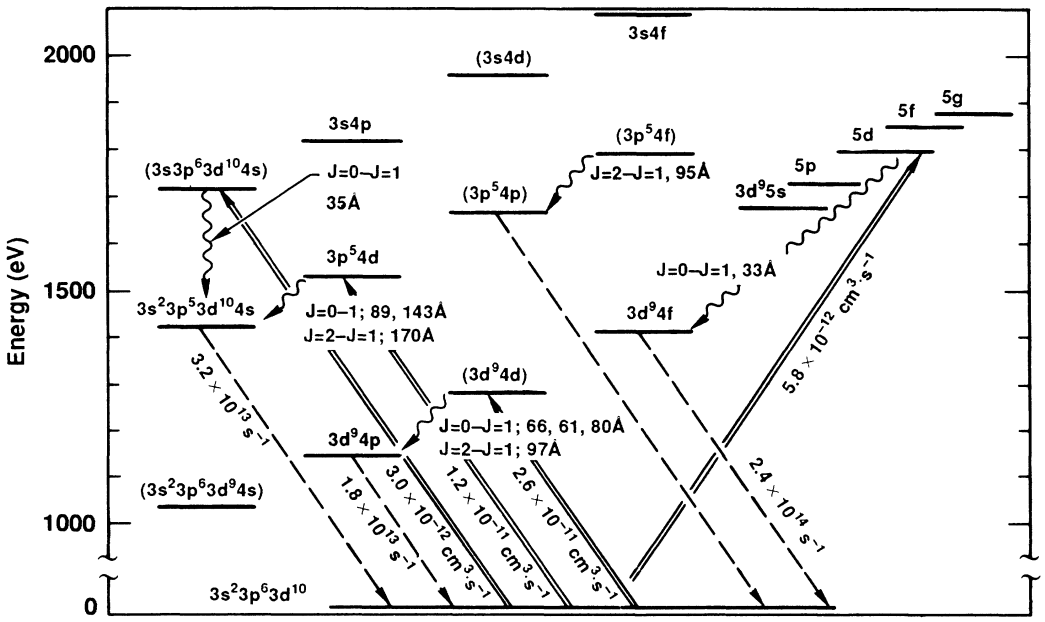

FIG. 1. Simplified level structure of the nickel-like ion. Configuration average energies for gadolinium are represented. Metastable configurations are given in parentheses. All lasing transitions listed in Table II are shown, as well as the $5d$-$4f$ transition mentioned at the close of Sec. III. Dashed lines show the resonance decays that drain population from lower levels; rates for these decays are given for the $J=0$ to $J=1$ transitions at 35, 89, 66, and 33 Å. Double lines show the important monopole collisional excitations. Note the energy overlap between $3d^9 5l$ configurations and states with inner-shell vacancies.

solved for the level populations n_j, both in the limit of an optically thin plasma and for the more realistic case including radiation trapping. The optically thin case focuses tightly on the collisional kinetics and is useful for studying the behavior of gain coefficients with changing electron density (as opposed to ion density). These results are also relevant to a hypothetical experiment that employs detrapping.[18]

For the optically thick plasma, we have modeled the radiation transport using a simple 0-dimensional escape factor treatment.[19] This involved self-consistently correcting the Einstein coefficients appearing in Eq. (1) by $A_{ij} \rightarrow \epsilon_{ij} A_{ij}$, where

$$\epsilon_{ij} = (1/\tau_{ij}\sqrt{\pi}) \int_{-\infty}^{\infty} \{1 - \exp[-\tau_{ij} \exp(-y^2)]\} dy \qquad (2)$$

is the "escape factor" and

$$\tau_{ij} = \frac{\pi e^2}{mc\sqrt{\pi}} \frac{2\sqrt{\ln 2}}{\Delta_D} f_{ij} n_i l \qquad (3)$$

is the optical depth at line center in the transition $j \rightarrow i$. Here $\Delta_D(T_I)$ is the Doppler width at ion temperature T_I, f_{ij} is the oscillator strength of the transition, n_i is the population density of the absorbing state, and l is the width of the plasma column. The coupled quantities n_i and ϵ_{ij} are determined by solving iteratively Eqs. (1) and (2) until convergence is attained in the level populations. The escape factor (and gain formula) we have adopted assumes a pure Doppler profile, since this is the dominant broadening mechanism under the plasma conditions conducive to x-ray lasing.

The conditions we chose were $T_I \approx \frac{2}{3} T_e$ and $N_{\text{Ni-like}} = f_{\text{Ni-like}} N_e / Z_{\text{avg}}$, with the nickel-like fraction, $f_{\text{Ni-like}} = 0.35$, and the average degree of ionization, $Z_{\text{avg}} = 36$, corresponding to nickel-like gadolinium. For the plasma column we assumed a width of 100 μm. These conditions led to about 70 optical depths in the strongest $3d$-$4f$ transition at $T_e = 750$ eV and $N_e = 5 \times 10^{20}$ cm^{-3}.

The absence from our model of recombination requires further discussion, since at the temperatures attained in the laser-produced plasmas used as x-ray laser media these processes can populate nickel-like excited states. In the following discussion, we take the electron temperature to be 750 eV, the value at which our gain calculations were performed. At temperatures much below this the nickel-like stage is not produced appreciably.[5] Of course, lower temperatures can be reached and population inversions might occur in the expanding, recombining plasma formed at late times. But we expect the density in this phase to be too low to obtain realistic gain.

We can try to estimate the magnitude of the effect of the processes we have neglected using standard approximation formulas for their rate coefficients.[20] For example, using detailed balance, Kramer's formula for photoionization yields a hydrogenic approximation for the rate of radiative recombination into the ith level of an ion from the ground state of the next higher ionization stage,

$$\beta^{\text{rad}}(i) \approx 5 \times 10^{-14} (Z^*/g_{Z^*+1}) x^{1.5} e^x E_1(x) ,$$

in cm^3/sec, where E_1 is the usual exponential integral,[21] $x = \Delta E(i)/T_e$, $\Delta E(i)$ is the binding energy of the ith level, Z^* is the net charge of the recombined ion, and g_{Z^*+1} is the statistical weight of the recombining ground state. Taking $\Delta E \approx 1600$ eV, appropriate to the lowest-lying excited state of nickel-like gadolinium, and $T_e = 750$ eV, $\beta^{\text{rad}}(i) \leq 1.9 \times 10^{-13}$ cm^3/sec. This should be compared to typical rate coefficients for collisional transitions out of the nickel-like ground state, especially those for excitation of the upper levels of lasing transitions. As suggested by those quoted in Fig. 1, the largest collisional rates exceed our upper bound on the radiative recombination rate by 2 orders of magnitude. Other ground-state excitation rates range from 10^{-13} to 10^{-11}. But for all but a handful at the highest energy, the *total* rate at which levels are collisionally populated exceeds $10^{-12} N_e$ sec^{-1} for $N_e \geq 10^{20}$, easily dominating the radiative recombination rate.

In a similar way Lotz's formula for collisional ionization[22] yields an estimate for the three-body recombination rate. In fact, it is not difficult to derive a hydrogenic scaling relationship between the Lotz three-body and Kramer radiative rates,

$$\beta^{3B}(i)/\beta^{\text{rad}}(i) = 1 \times 10^{-14} (2n^2/Z^*) \times (T_e)^{-1/2} [\Delta E(i)]^{-2.5} ,$$

in cm^3, where T_e and ΔE are in eV and n is the principal quantum number of the ith state. For $n = 5$ and $T_e = 750$ eV, this ratio is $\approx 4 \times 10^{-23}$ cm^3, implying that the three-body and radiative rates become comparable only at densities $\geq 10^{22}$ cm^{-3}.

These estimates show that we are justified in neglecting radiative and three-body recombination under the plasma conditions that are expected to generate appreciable gain in nickel-like transitions. In Table I we collect collisional excitation, and radiative and three-body recombination rates for representative excited states of nickel-like gadolinium, including several of those that are involved in population inversions. Only recombination from the $(3d^9)_{3/5,5/2}$ ground states of the cobalt-like ion is included, with the assumption that these nearly degenerate states are populated statistically with respect to each other. The radiative rates were obtained by detailed balancing hydrogenic photoionization cross sections and assuming statistical branching ratios. Three-body rates are from a detailed balancing of Lotz's formula. Of the three processes, collisional excitation is clearly dominant under the plasma conditions investigated here.

Dielectronic recombination, however, is not so easily disposed of. Based on calculations by Chen for dielectronic recombination from nickel-like to copper-like gadolinium,[23] we expect the total rate coefficient for cobalt-like to nickel-like recombination to be $\cong 10^{-10}$ cm^3/sec for $T_e \leq 1$ keV. It is possible, then, that recombination rates into individual excited nickel-like levels are comparable to typical collisional pumping rates, assuming comparable concentrations of nickel-like and cobalt-like ions. Unfortunately, accurate level-to-level rates for dielectronic recombination from cobalt-like to nickel-like ions are neither readily available nor calculable. (The crude rates

TABLE I. Rates (sec^{-1}) at $N_e = 5\times10^{20}$ cm^{-3} and $T_e = 750$ eV of ground-state collisional excitation, and radiative and three-body recombination into representative excited levels of nickel-like gadolinium. Levels that are nearer to J-J coupling are denoted by $[(nl_j)n'l'_j]_J$, where the vacancy is indicated in parentheses. Values were obtained by the methods described in Sec. II. The last column gives the rate at which population is destroyed by collisional processes.

Level	Collisional excitation	Radiative recombination	Three-body recombination	Collisional destruction
$3d^9 4d(^1S_0)$	1.3×10^{10}	6.5×10^{6}	7.3×10^{3}	1.6×10^{12}
$[(3d_{3/2})4p_{1/2}]_1$	8.0×10^{8}	1.8×10^{7}	1.7×10^{4}	1.5×10^{12}
$[(3d_{3/2})4p_{3/2}]_1$	2.4×10^{8}	1.9×10^{7}	1.7×10^{4}	1.6×10^{12}
$[(3d_{5/2})4p_{3/2}]_1$	1.5×10^{9}	1.9×10^{7}	1.8×10^{4}	1.6×10^{12}
$[(3d_{5/2})4d_{5/2}]_2$	8.5×10^{8}	3.1×10^{7}	3.4×10^{4}	1.4×10^{12}
$[(3d_{5/2})4f_{7/2}]_6$	4.9×10^{8}	3.1×10^{7}	1.0×10^{5}	8.1×10^{11}
$[(3d_{5/2})5g_{9/2}]_7$	2.4×10^{7}	5.7×10^{6}	2.8×10^{5}	2.0×10^{12}

used recently by Maxon *et al.*[7] were obtained by scaling a hydrogenic calculation both in Z and in isoelectronic sequence, together with a statistical assumption for the branching ratios into detailed levels.) Work is presently underway on this calculation by us and others.[24]

In the meantime, the present model is advanced as an accurate, detailed, and extensive treatment focusing on collisional excitation as the mechanism for producing nickel-like population inversions. This approach is further justified by the strong probability that the plasma conditions obtained in recent experiments fall within its scope.[8] In any case, using the neon-like system as a guide,[13,14] we do not expect dielectronic recombination to effect the inversion of $J=0$ to $J=1$ transitions under any circumstances; while for $J=2$ to $J=1$ inversions, the gain obtained from collisional excitation can safely be treated as a lower bound.

Recombination can destroy population in nickel-like excited states as well as create it. If we assume that the values for the cobalt-like to nickel-like processes can serve as estimates for nickel-like to copper-like radiative and three-body recombination, they can be compared to the rate at which the excited-state population is destroyed by internal collisional transitions. Representative collisional destruction rates at $N_e = 5\times10^{20}$ cm^3 are given in Table I. These comfortably exceed the estimated radiative and three-body rates at the same density, and, in fact, also dominate dielectronic recombination, as calculated by Chen.[23]

In contrast to recombination, collisional ionization is not expected to appreciably populate nickel-like excited states. This is because at the relevant temperatures valence-shell ionization is dominant,[25] while excited levels are directly fed only through inner-shell ionization of copper-like and zinc-like ions. Of course, as in the neon-like system, the effects of inner-shell ionization[4,14]—by suprathermal electrons, for example[4]—on nickel-like population inversions are worth investigation in their own right. Calculations of detailed level-to-level rate coefficients for the ionization of copper-like to nickel-like ions are presently underway.[25]

III. GAIN PREDICTIONS

The small-signal gain coefficient for the transition $i\rightarrow j$ is given by

$$\alpha_{ij} = (\lambda_{ij}^3 A_{ij}/8\pi)\sqrt{(M_I/2\pi k_B T_I)}\, g_i W_{ij} ,$$

for pure Doppler broadening, where k_B is Boltzmann's constant, M_I is the atomic weight of the ion, g_i is the statistical weight of state i, and W_{ij} is the population inversion,

$$W_{ij} = n_i/g_i - n_j/g_j .$$

We have calculated the gain coefficient under a range of plasma conditions for the transitions listed in Table II. The letter key associated with each transition is for use with Figs. 2–5. The wavelengths quoted in Table II are theoretical and, judging by past efforts to calculate the positions of $\Delta n = 0$ lines *ab initio*, may undershoot by up to 5%. We have included in Table II the optical depths in the lines that drain the lower level of each transition, at an ion density of 5×10^{18} cm^{-3}.

In Fig. 2 are presented gain coefficients at $T_e = 750$ eV as a function of density for the $3d^9 4d(J=0)$-$3d^9 4p(J=1)$ transitions. Dashed lines represent the optically thin calculation, while the solid curves show the effect of radiation trapping in the approximation and under the conditions described in Sec. II. The importance of trapping in limiting the gain that can be obtained on nickel-like transitions is very clear in this figure.

It is worth noting that the three transitions shown in Fig. 2 have the same upper level, fed by a strong monopole excitation from the $3d^{10}$ ground state. This explains the parallel behavior of the gain coefficients at low density, and in the optically thin limit. The population in their various lower levels is trapped at different ion densities, however, leading to the dissimilar behavior of the optically thick case. For the strongest transition, A, analogous to the one observed recently at 71 Å in europium, we have obtained gain coefficients for

TABLE II. Lasing transitions in nickel-like gadolinium. Level nomenclature is identical to that used in Table I. Wavelengths are calculated in the relativistic multiconfigurational parametric potential model. The number of optical depths in the lower state is given for a 100-μm diameter plasma at $T_I = 450$ eV, $N_I = 5 \times 10^{18}$ cm^{-3}. The letter key is for use with the text and figures.

Key	Upper level	Lower level	Wavelength (Å)	Optical depth (τ)
		$3d^9 4d$-$3d^9 4p$		
A	$3d^9 4d(^1S_0)$	$[(3d_{5/2})4p_{3/2}]_1$	66.5	4.34
B	$3d^9 4d(^1S_0)$	$[(3d_{3/2})4p_{1/2}]_1$	61.5	1.74
C	$3d^9 4d(^1S_0)$	$[(3d_{3/2})4p_{3/2}]_1$	79.7	0.51
D	$[(3d_{5/2})4d_{5/2}]_2$	$[(3d_{5/2})4p_{3/2}]_1$	97.4	4.34
		$3p^5 3d^{10} 4l$-$3p^5 3d^{10} 4l'$		
E	$[(3p_{3/2})4p_{3/2}]_0$	$[(3p_{3/2})4s]_1$	89.6	4.54
F	$[(3p_{1/2})4p_{1/2}]_0$	$[(3p_{1/2})4s]_1$	143.7	0.55
G	$[(3p_{3/2})4p_{1/2}]_2$	$[(3p_{3/2})4s]_1$	168.8	4.54
H	$[(3p_{3/2})4f_{7/2}]_2$	$[(3p_{3/2})4d_{5/2}]_1$	95.1	11.00
I	$[(3p_{1/2})4f_{5/2}]_2$	$[(3p_{1/2})4d_{3/2}]_1$	94.7	4.47
		$n = 3$-$n = 3$		
J	$[(3s)4s]_0$	$[(3p_{3/2})4s]_1$	35.6	4.54
K	$[(3p_{3/2})4p_{3/2}]_0$	$[(3d_{5/2})4p_{3/2}]_1$	34.1	4.34
L	$[(3s)4s]_0$	$[(3p_{1/2})4s]_1$	62.1	0.55

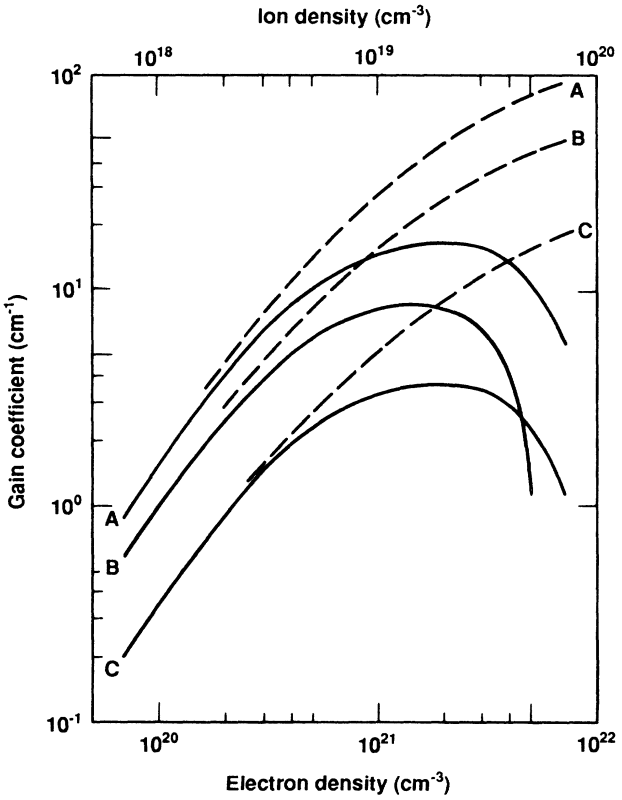

FIG. 2. Predicted gain coefficient (cm^{-1}) as a function of electron density (cm^{-3}) at $T_e = 750$ eV, for $3d^9 4d(J=0)$-$3d^9 4p(J=1)$ transitions. Dashed curves represent the optically thin limit. The solid curves refer to a calculation that included line trapping in the escape-factor approximation, for a 100-μm diameter plasma with $T_I = 450$ eV. In this and subsequent figures the ion density is the density of nickel-like ions under the conditions described in Sec. II.

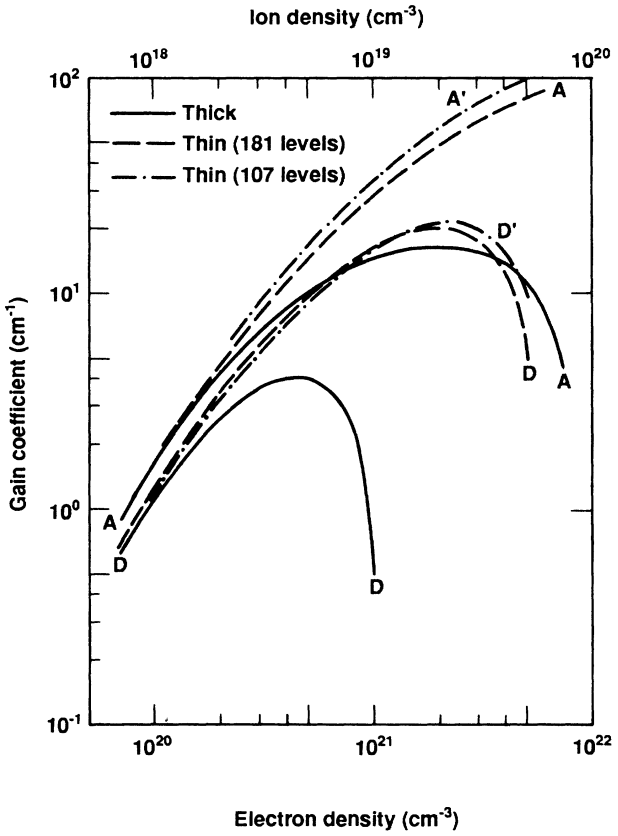

FIG. 3. Comparison of predicted gain coefficient for $4d(J=0)$-$4p(J=1)$ at 66 Å with that of $J=2$ to $J=1$ at 97 Å. Calculations with and without trapping are represented as in Fig. 2. The dashed curves labeled *A'* and *D'* show the results of using a 107-level model.

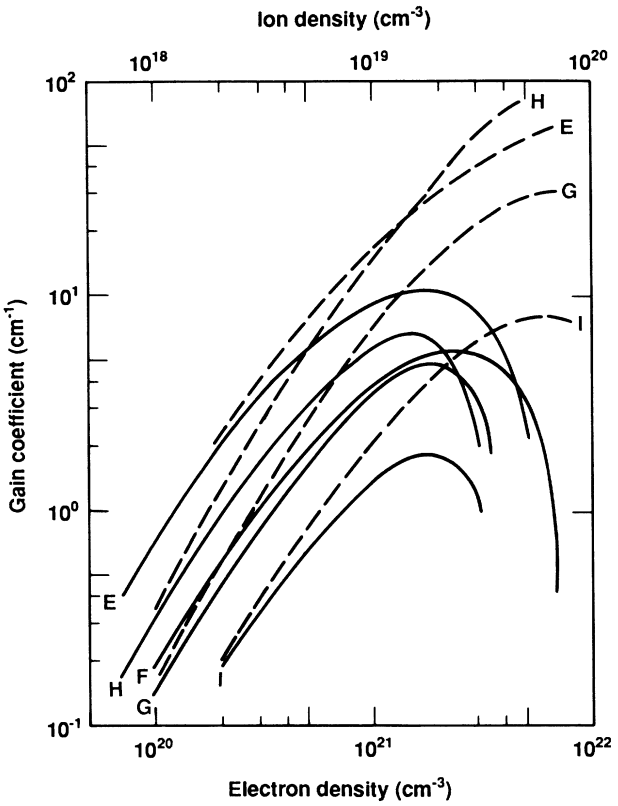

FIG. 4. Predicted gain coefficients for $n=4$ to $n=4$ transitions with a spectator vacancy in the $3p$ orbital. Conditions for the calculations with and without trapping are the same as in Fig. 2.

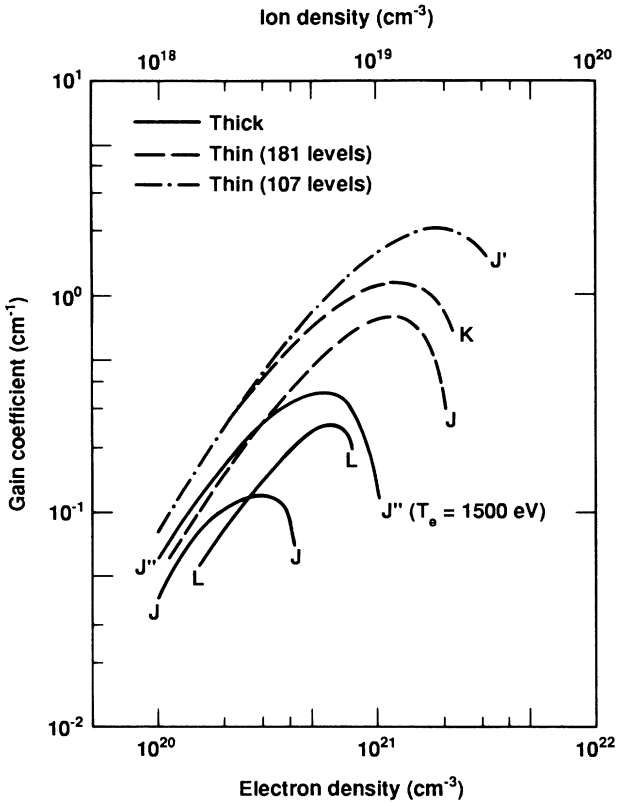

FIG. 5. Predicted gain coefficients for $n=3$ to $n=3$ transitions. Solid and dashed curves represent the same conditions as in Fig. 2, except the curve labeled J'', for which $T_e=1500$ eV and $T_I=1000$ eV. The dashed curve labeled J' is a calculation in the 107-level model.

$N_e \approx 3-5\times 10^{20}$ that are in fair agreement with previous kinetics calculations,[5] and with the peak gains predicted in recent design studies.[7]

In Fig. 3 we compare the strongest $3d^9 4d\,(J=2)$-$3d^9 4p\,(J=1)$ transition, D observed without gain in the recent experiment,[8] to the A line. These transitions share the same lower level. The $J=2$ to $J=1$ line is amplified significantly less, and over a smaller range of densities, than the $J=0$ to $J=1$, at least when, as here, collisional excitation only is taken into account. This is consistent with the recent design calculation which found that dielectronic recombination is primarily responsible for the $J=2$ to $J=1$ inversion.[7] That gain is not observed on this transition is consistent with a conclusion that recombination does not play an important role in the lasing plasma (either because the plasma conditions differ from those of the simulation, or because the recombination rates were inaccurate).[26]

Comparing the solid and dashed (optically thick and thin) curves in Fig. 3, we see that trapping has apparently a greater relative effect on the $J=2$ to $J=1$ gain than on the $J=0$ to $J=1$. Since these transitions have the same trapped lower level, this difference can be traced to the simple fact that the $J=2$ to $J=1$ inversion is smaller in the optically thin limit: if $\Delta W_{ij}=W_{ij}^{\text{thin}}-W_{ij}^{\text{thick}}$, then

$$[(\Delta W_{0\text{-}1}/W_{0\text{-}1}^{\text{thin}})/(\Delta W_{2\text{-}1}/W_{2\text{-}1}^{\text{thin}})]\approx W_{2\text{-}1}^{\text{thin}}/W_{0\text{-}1}^{\text{thin}}\ .$$

We have also displayed, as the curves labeled A' and D' in Fig. 3, the results of an optically thin calculation using a 107-level model. The less complete model *overestimates* the gain on the $J=0$ to $J=1$ transition because of two effects. First, without the opportunity to transfer population into the $n=5$ states, the upper level is collisionally depopulated at a slower rate. Second, there is about a 7% reduction in the monopole excitation rate in the larger model owing to configuration interaction between the $3d^9 4d(J=0)$ and $3d^9 5d(J=0)$ states. Although this effect is nearly negligible here, we will see that it plays an important role for inner-shell transitions.

For the $J=2$ to $J=1$ transition, at lower densities the gain is slightly *underestimated* in the smaller model since it does not include cascades from $n=5$ manifolds. Once the transition is collisionally quenched, above $N_e=10^{21}$ cm^{-3} or so, by population transfer out of the upper and into the lower level, the larger model—which accelerates this process—predicts a significantly lower gain.

For $N_e=5\times 10^{20}$ we obtain a value of 0.4 for the ratio of the $J=2$ to $J=1$ gain to the $J=0$ to $J=1$ gain. A previous calculation that also neglected recombination found a ratio 50% larger under similar, but slightly more optically thick, conditions.[5] (Note that increased trapping should decrease the ratio.) A reasonable hypothesis is that the lower ratio is attributable to the inclusion in the present model of all $\Delta n=0$ collisional transitions.

Previous models included only the dipole-allowed excitations, since only these transitions are computable in the classical path approximation. The consequent increase in collisional population transfer reduces the gain on the $J=2$ to $J=1$ line. Of course, it is also possible that the dipole-allowed rates differ between the classical path and distorted-wave approximations.

The gain coefficients for $n=4$ to $n=4$ transitions that involve a spectator hole in the $3p$ shell are displayed in Fig. 4. E and F denote $J=0$ to $J=1$ lines, and G, H, and I, $J=2$ to $J=1$ lines. Here again, a comparison of the E and G transitions—which share a $3p^5 4s$ lower level—with and without optical depth demonstrates the greater relative importance for the $J=2$ to $J=1$ inversions of line trapping.

Figure 5 shows gain coefficients for $n=3$ to $n=3$ transitions, presented here for the first time. The most interesting of these is J, a $3p$-$3s$ inversion that radiates within the water window and shows signs of surviving line trapping. The $3d$-$3p$ line denoted by K also lies below 44 Å, and has a larger gain coefficient than J in the optically thin limit, but trapping effectively destroys this inversion.

We have displayed four curves in Fig. 5 for the $3p$-$3s$ transition. The solid curve labeled J represents the gain coefficient at $T_e=750$ eV. The sensitivity of this inversion to temperature is evident from the J'' curve, calculated at $T_e=1500$ eV and $T_1=1000$ eV. The strong dependence on temperature here—not observed in $n=4$ to $n=4$ transitions—can be traced to the threshold energy of over 1700 eV for exciting the upper level. In fact, the gain for this line saturates around 2 keV. As usual, the dashed curve—also labeled J—represents the optically thin limit (at $T_e=750$ eV). Here it illustrates the catastrophic effects of trapping on inner-shell inversions.

The dashed curve denoted J' in Fig. 5 illustrates the importance of including the $n=5$ states in the calculation. Evidently, an important factor of 2 in the gain is lost in the more complete model. The source of this reduction in gain is the configuration interaction between the $3s3p^6 3d^{10} 4s\,(J=0)$ and $3s^2 3p^6 3d^9 5d\,(J=0)$ states. The $3p\,(J=0)$-$3s\,(J=1)$ inversion is fed, in the standard way, by a strong monopole excitation from the ground state. In the smaller model, the rate coefficient for this excitation is 4.3×10^{-12} cm^{-3}/sec at $T_e=750$ eV, but mixing with the $5d$ states reduces this by $\frac{1}{3}$.

An interesting corrollary of this effect is that the population of the $3d^9 5d\,(^1S_0)$ state is inverted with respect to the $3d^9 4f\,(^1P_1)$, providing an unusual example of a *collisionally* pumped $\Delta n=1$ amplified transition. This line, calculated at 32.9 Å in gadolinium, has a peak gain of over 0.5 cm^{-1} in the optically thin limit. Of course, in reality the lower level is severely trapped by reabsorption.

IV. CONCLUSIONS

We have modeled the nickel-like charge state by 181 low-lying levels, including the $3d^9 5l$ configurations. All collisional transition rates were included in the distorted-wave approximation, as well as all $E1$, $E2$, and $M2$ radiative rates. Ionization and radiative and three-body recombination were omitted because they play a negligible role in populating nickel-like excited states in the lasing plasma. Dielectronic recombination was also not included in the model, though it may be important under some circumstances. When reliable dielectronic rates become available, they will be added to the present model. In the meantime, recently reported experimental results[8] apparently reflect plasma conditions that suppress dielectronic recombination and, therefore, fall within the scope of our model. Plasma conditions were taken to be homogeneous and time-independent in order to focus on the population kinetics independently of design issues. Line trapping was included in a 0-dimensional escape-factor approximation.

We found that the $3d^9 5l$ states effect the kinetics through cascades, and by increasing the collisional redistribution of population. The latter effect significantly reduces the gain of the $3d\,(J=2)$-$3p\,(J=1)$ transition at high densities, while the former augments it marginally at lower densities. Overall, we find a lower gain for this transition, relative to the observed $J=0$ to $J=1$ line, than has been previously calculated, probably owing to more complete accounting of collisional population transfer.

By comparing optically thin with optically thick calculations of gain coefficients, we saw that line trapping has a greater impact on the $J=2$ to $J=1$ transition, relative to the $J=0$ to $J=1$. This was also concluded from recent design studies.[7] However, this result could be traced to the smaller "initial"—that is, optically thin—inversion for this line, rather than to a difference in the effect on the kinetics of the two inversions. This is not surprising, since the two transitions share their lower level. Trapping could, therefore, help explain the experimental absence of the $J=2$ to $J=1$ line, but only in a scenario where the line was kinetically supressed anyway, as when dielectronic recombination is unimportant.

In addition to the standard $n=4$ to $n=4$ population inversions, we have studied the behavior of inner-shell, $n=3$ to $n=3$, transitions. Two of these have wavelengths below 44 Å in nickel-like gadolinium, hinting at the tantalizing possibility of breaking the water window with relatively low-Z elements. Unfortunately these inversions are particularly sensitive to trapping and lose $\frac{2}{3}$ or more of their peak gain under the conditions we assumed. To add insult to injury, the 35-Å, $3p\,(J=0)$-$3s\,(J=1)$, line that apparently survives the line trapping, is subject to an egregious configuration interaction with the $3d^9 5d\,(^1S_0)$ state. This interaction reduces the rate for the monopole excitation that feeds the transition's upper level by $\frac{1}{3}$, lowering the peak gain to just over 0.1 cm^{-1}. Still, this peak occurs in just the right density regime, around 3×10^{20} cm^{-3}, for current experimental designs. (It is also worth noting that a 5% undershoot on the wavelength calculation—a good guess—would lead to a 15% increase in predicted gain.)

Since configuration interaction can be quite sensitive to Z, it is possible that a Z-scaling study might identify an element for which the effect of configuration interaction on the $3p\,(J=0)$-$3s\,(J=1)$ line is minimized, while its wavelength remains below 44 Å. We plan to do this study, and will report further if results are favorable.

ACKNOWLEDGMENTS

The authors thank S. Maxon for helpful discussions on the results on his design calculations, and M. Chen for valuable comments on dielectronic recombination. This work was performed under the auspices of the U.S. Department of Energy by Lawrence Livermore National Laboratory under Contract No. W-7405-Eng-48.

---

*Permanent address: Nuclear Research Center of the Negev, P.O. Box 9001, Beer Sheva, Israel.

[1]D. L. Matthews *et al.*, Phys. Rev. Lett. **54**, 110 (1985).

[2]A. V. Vinogradov, I. Skobelev, and E. A. Yukov, Kvant. Elektron. (Moscow) **3**, 981 (1976) [Sov. J. Quant. Electron. **6**, 525 (1976)]; L. J. Palumbo and R. C. Elton, J. Opt. Soc. Am. **67**, 480 (1977); J. P. Apruzese, P. C. Kepple, J. Davis, and J. Pender, in Proceedings of the Sixth American Physical Society Topical Conference on Atomic Processes in High-Temperature Plasmas and International Conference/Workshop on the Radiative Properties of Hot Dense Matter, Santa Fe, 1987 (unpublished).

[3]P. Jaegle *et al.*, Phys. Rev. Lett. **18**, 1070 (1974); J. C. Gauthier, J. P. Geindre, N. Grandjouan, and J. Virmont, J. Phys. D **16**, 321 (1983); A. Sureau, H. Guennon, and M. Cornille, J. Phys. B **17**, 541 (1984); G. Jamelot, A. Klisnick, A. Carillon, H. Guennon, A. Sureau, and P. Jaegle, J. Phys. B **18**, 4647 (1985); P. Jaegle, A. Carillon, A. Klisnick, G. Jamelot, H. Guennou, and A. Sureau, Europhys. Lett. **1**, 555 (198); B. L. Whitten, J. K. Nash, A. L. Osterheld, M. H. Chen, in Proceedings of the Sixth American Physical Society Topical Conference on Atomic Processes in High-Temperature Plasmas and International Conference/Workshop on the Radiative Properties of Hot Dense Matter, Santa Fe, 1987 (unpublished); G. Jamelot, A. Klisnick, A. Carillon, B. Gauthe, F. Gadi, and P. Jaegle, *ibid.*

[4]W. H. Goldstein and R. S. Walling, Phys. Rev. A **36**, 3482 (1987).

[5]S. Maxon, P. Hagelstein, J. Scofield, and Y. Lee, J. Appl. Phys. **59**, 294 (1986); S. Maxon, P. Hagelstein, K. Reed, and J. Scofield, *ibid.* **57**, 971 (1985).

[6]A. Zigler, M. Klapisch, and A. Bar-Shalom, in Conference on Atomic Processes in Hot Dense Plasmas, Jerusalem, 1986 (unpublished).

[7]S. Maxon *et al.*, Phys. Rev. A **37**, 2227 (1988).

[8]B. J. MacGowan *et al.*, Phys. Rev. Lett. **59**, 2157 (1987).

[9]M. D. Rosen *et al.*, Phys. Rev. Lett. **54**, 106 (1985).

[10]M. D. Rosen (private communication).

[11]B. MacGowan *et al.*, J. Appl. Phys. **61**, 5243 (1987).

[12]T. N. Lee, E. A. McLean, and R. C. Elton, Phys. Rev. Lett. **59**, 1185 (1987).

[13]B. L. Whitten, A. U. Hazi, M. H. Chen, and P. L. Hagelstein, Phys. Rev. A **33**, 2171 (1986).

[14]W. H. Goldstein, B. L. Whitten, A. U. Hazi, and M. H. Chen, Phys. Rev. A **36**, 3607 (1987).

[15]ANGLAR is a computer program for calculating angular coefficients of atomic matrix elements. It is based on the program of I. Grant, Comput. Phys. Commun. **5**, 263 (1973). Grant's program was modified to evaluate coefficients using graphical methods by A. Bar-Shalom and M. Klapisch, "NJGRAF—An efficient program for calculation of general recoupling coefficients by graphical analysis compatible with NJSYM," Comput. Phys. Commun. (to be published).

[16]RELAC is a relativistic version of the parametric potential-based atomic structure program MAPAC; M. Klapisch, Comput. Phys. Commun. **2**, 239 (1971). RELAC was introduced and described by M. Klapisch, J. L. Schwob, B. S. Fraenkel, and J. Oreg, J. Opt. Soc. Am. **61**, 148 (1977).

[17]A. Bar-Shalom, M. Klapisch, and J. Oreg, Phys. Rev. A (to be published).

[18]See, for example, J. G. Lunney, Opt. Commun. **53**, 235 (1985); R. C. Elton, Naval Research Laboratory Report No. 5906, 1986 (unpublished), and references therein; Proceedings of the X-87 International Conference on X-ray and Innershell Processes [J. Phys. (to be published)].

[19]C. Breton and J. L. Schwob, C. R. Acad. Sci. Paris **260**, 461 (1965); J. L. Schwob, Commissariat à l'Energie Atomique Report No. CEA-R-3359 EUR. 3579f, 1969 (unpublished). The escape factor introduced by Schwob is a spatial average assuming a homogeneous plasma, with the path of each photon taken into account. It represents an improvement over the more familiar approach that assumes that photons are emitted only at the center of the plasma and absorbed by the surrounding medium. Schwob's approach tends to yield less trapping under given conditions. Descriptions and comparisons of the various escape factor treatments of line trapping can be found in F. E. Irons, J. Quant. Spectrosc. Radiat. Transfer **22**, 1 (1979).

[20]I. I. Sobelman, L. A. Vainshtein, and E. A. Yukov, *Excitation of Atoms and Broadening of Spectral Lines* (Springer-Verlag, Berlin, 1981); J. C. Weisheit, Lawrence Livermore National Laboratory Report No. UCID-20744, 1986 (unpublished).

[21]See, for example, *Handbook of Mathematical Functions*, edited by M. Abramowitz and I. A. Stegun (Dover, New York, 1965).

[22]W. Lozt, Astrophys. J. Suppl. **14**, 207 (1967).

[23]M. H. Chen, Phys. Rev. **35**, 4129 (1987).

[24]M. H. Chen (private communication).

[25]D. Sampson (private communication).

[26]Recent work by S. Maxon suggests that the plasma obtained in rare-earth exploding foil experiments is less highly ionized than predicted by hydrodynamic simulation (private communication).